

UC Irvine

UC Irvine Previously Published Works

Title

Electronic inhomogeneity in a Kondo lattice

Permalink

<https://escholarship.org/uc/item/18b8r71k>

Journal

Proceedings of the National Academy of Sciences of the United States of America, 108(17)

ISSN

0027-8424

Authors

Bauer, ED
Yang, Yi-feng
Capan, C
et al.

Publication Date

2011-04-26

DOI

10.1073/pnas.1103965108

Copyright Information

This work is made available under the terms of a Creative Commons Attribution License, available at <https://creativecommons.org/licenses/by/4.0/>

Peer reviewed

Electronic inhomogeneity in a Kondo lattice

E. D. Bauer^{a,1}, Yi-feng Yang^{a,b,1}, C. Capan^c, R. R. Urbano^d, C. F. Miclea^a, H. Sakai^e, F. Ronning^a, M. J. Graf^a, A. V. Balatsky^a, R. Movshovich^a, A. D. Bianchi^f, A. P. Reyes^d, P. L. Kuhns^d, J. D. Thompson^a, and Z. Fisk^{c,1}

^aLos Alamos National Laboratory, Los Alamos, NM 87545; ^bInstitute of Physics, Chinese Academy of Sciences, Beijing 100190, China; ^cDepartment of Physics and Astronomy, University of California, Irvine, CA 92697; ^dNational High Magnetic Field Laboratory, Florida State University, Tallahassee, FL 32306; ^eAdvanced Science Research Center, Japan Atomic Energy Agency, Tokai, Ibaraki 319-1195, Japan; and ^fDepartment de Physique, Université de Montréal, Montréal, QC, Canada H3C 3J7

Contributed by Zachary Fisk, March 15, 2011 (sent for review December 29, 2010)

Inhomogeneous electronic states resulting from entangled spin, charge, and lattice degrees of freedom are hallmarks of strongly correlated electron materials; such behavior has been observed in many classes of *d*-electron materials, including the high- T_c copper-oxide superconductors, manganites, and most recently the iron-pnictide superconductors. The complexity generated by competing phases in these materials constitutes a considerable theoretical challenge—one that still defies a complete description. Here, we report a manifestation of electronic inhomogeneity in a strongly correlated *f*-electron system, using CeCoIn₅ as an example. A thermodynamic analysis of its superconductivity, combined with nuclear quadrupole resonance measurements, shows that nonmagnetic impurities (Y, La, Yb, Th, Hg, and Sn) locally suppress unconventional superconductivity, generating an inhomogeneous electronic “Swiss cheese” due to disrupted periodicity of the Kondo lattice. Our analysis may be generalized to include related systems, suggesting that electronic inhomogeneity should be considered broadly in Kondo lattice materials.

Kondo effect | heavy fermion

Electronic inhomogeneity is commonplace in materials in which strong correlations among electrons produce electronic states that compete with one another on multiple length scales (1). One early indication of such heterogeneity came from studies of the high- T_c cuprate superconductors in which nonmagnetic Zn impurities were introduced into the CuO₂ planes of YBa₂Cu₃O_{6+x} (YBCO) and La_{2-x}Sr_xCuO₄ (LSCO)²; the anomalous suppression of the superfluid density of the superconducting condensate was explained within a Swiss cheese model comprised of normal regions around the impurity that healed over a (short) coherence length of order 20 Å within a superconducting matrix (2), later verified by scanning tunneling spectroscopy (3). Not only is superconductivity locally suppressed in the Swiss cheese regions, but new electronic states emerge, such as impurity resonances and other exotic forms of electronic inhomogeneity (e.g., “stripe” and “checkerboard” phases) observed in cuprates and also in other *d*-electron materials (e.g., manganites) (1, 4). In contrast, electronic inhomogeneity has rarely been considered in the prototypical correlated system: *f*-electron materials (5) in which itinerant heavy quasiparticles emerge at low temperature due to a periodic lattice of Kondo ions. In this work, we investigate the underlying electronic structure of the Kondo lattice compound CeCoIn₅ whose heavy quasiparticles pair to create a *d*-wave superconducting state below 2.3 K (6). As will be discussed, the superconductivity itself serves as a mirror that reflects the presence of electronic inhomogeneity. A thermodynamic analysis of high-purity single crystals of CeCoIn₅, doped with different impurities (Y³⁺, La³⁺, Yb²⁺, Th⁴⁺, Hg, and Sn), reveals that lattice sites filled by these impurities create “Kondo holes” (7, 8) that produce a nonsuperconducting component within the superconducting state, very much like the Swiss cheese model of the cuprates (2). Our results not only provide strong evidence for an inhomogeneous electronic ground state in this *f*-electron heavy fermion superconductor, they uncover fundamental properties of the Kondo lattice itself.

Results and Discussion

Substitutions for Ce (or In) in CeCoIn₅ by nonmagnetic elements R (or Hg, Sn) rapidly suppress T_c , with $T_c \rightarrow 0$ K typically in the range of 10–15% substitution for Ce (In). Fig. 1 shows that, concomitant with the depression of T_c , there is a systematic increase in the value of C/T ($T \rightarrow 0$ K) $\equiv \gamma_0$ that is a measure of a non-superconducting electronic contribution to specific heat in the superconducting state. In a magnetic field of $H = 5$ T ($H \parallel c$ axis), the normal state Sommerfeld coefficient γ_N follows a logarithmic temperature dependence, indicating proximity to a quantum critical point (9) for all dopants. An extrapolation of the infield C/T data to $T = 0$ K, such that the extrapolation conserves entropy between the normal and superconducting states at T_c , yields $\gamma_N > 1.2$ J/mol Ce K² for all concentrations. We make the ansatz that there is an additional normal component to C/T below T_c given by γ_0/γ_N and compare this normal component to the reduction of the superconducting condensation energy $R_U = [U_{SC}(x)/T_c^2(x)]/[U_{SC}(0)/T_c^2(0)]$ (properly normalized relative to the condensation energy of pure CeCoIn₅), where $U_{SC} = \int_0^{T_c} (S_N - S_{SC})dT$. As shown in Fig. 2A, the doping-induced normal state fraction comes *precisely* at the expense of the superconducting state fraction as evidenced by a common linear variation of $R_\gamma = \gamma_0/\gamma_N$ vs. $1 - R_U$, for all substituents (Y³⁺, La³⁺, Th⁴⁺, Yb²⁺, Hg, and Sn—see Fig. 2B and Fig. S1), regardless of valence or size of the impurity atom. This unexpected result provides compelling evidence for electronic inhomogeneity in an *f*-electron Kondo lattice. Furthermore, the linear dependence of γ_0/γ_N on impurity concentration (Fig. 2A, *Inset*) does not follow the expectation for creating electronic states in superconducting nodes through disorder in a “dirty” *d*-wave scenario in the strong scattering (unitary) limit (for which $\gamma_0/\gamma_N \sim x^{1/2}$) or in the weak scattering (Born) limit (Fig. 3A), implying that the impurities suppress the superconducting energy gap through the creation of intragap states, much like Zn impurities in YBCO and Bi₂Sr₂CaCu₂O_{8+δ} (Fig. 3B) (4, 10). In this analysis, we have used the simple Bardenheer–Schrieffer expression for the condensation energy $U_{SC} = N(0)\Delta^2/2 \sim T_c^2$, where $N(0)$ is the density of states at the Fermi level, to allow a comparison of the different dopants substituted into the heavy fermion superconductors. More complete calculations of U_{SC} for unitary scatterers is plotted as γ_0/γ_N vs. $1 - U_{SC}(\Gamma)/U_{SC}(0)$ in Fig. S2, where Γ is the impurity scattering rate. These calculations do not reproduce the universal linear relation of R_γ vs. $1 - R_U$ (Fig. 2B), furthering a scenario of electronic heterogeneity in which the dopants locally suppress superconductivity.

Author contributions: J.D.T. and Z.F. designed research; E.D.B., C.C., R.R.U., C.F.M., H.S., F.R., M.J.G., A.V.B., R.M., A.D.B., A.P.R., and P.L.K. performed research; E.D.B., C.C., and A.D.B. prepared samples; E.D.B., Y.-f.Y., C.C., R.R.U., C.F.M., H.S., F.R., R.M., A.D.B., and A.P.R. analyzed data; and E.D.B. and Y.-f.Y. wrote the paper.

The authors declare no conflict of interest.

¹To whom correspondence may be addressed. E-mail: edbauer@lanl.gov, yifeng@iphy.ac.cn, or zfsk@uci.edu.

This article contains supporting information online at www.pnas.org/lookup/suppl/doi:10.1073/pnas.1103965108/-DCSupplemental.

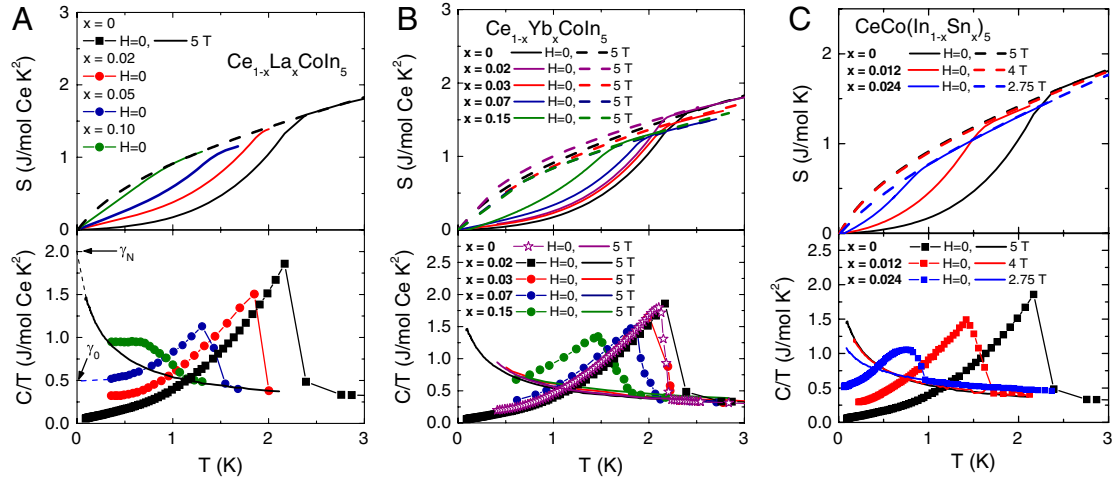


Fig. 1. Specific heat coefficient and entropy of CeCoIn_5 when nonmagnetic impurities (La, Yb^{2+}) replace Ce or when In is replaced by Sn or Hg in the crystal lattice. Specific heat, plotted as $C(T)/T$ (Lower), and entropy $S(T) = \int (C/T) dT$ (Upper), of $\text{Ce}_{1-x}\text{R}_x\text{CoIn}_5$ (A) $\text{R} = \text{La}^{3+}$ (28), (B) $\text{R} = \text{Yb}^{2+}$, and (C) $\text{CeCo}(\text{In}_{1-x}\text{Sn}_x)_5$ showing the suppression of superconductivity and the increase of the residual superconducting state specific heat coefficient γ_0 determined from a linear extrapolation of the C/T data to $T = 0$ K, consistent with a superconducting gap with lines of nodes observed previously (6). The normal state Sommerfeld coefficient γ_N was determined from a linear extrapolation of the C/T data to $T = 0$ K that balances entropy between the normal and superconducting states as shown in the upper panels of A, B, and C. The dashed lines in the lower panel of A are an example of the extrapolation of the C/T data used to determine γ_0 and γ_N for the $\text{Ce}_{0.95}\text{La}_{0.05}\text{CoIn}_5$ sample.

Our thermodynamic analysis of impurities introduced into CeCoIn_5 further implies that the electronic inhomogeneity arises from disruption of the coherent Kondo lattice by Kondo holes. We estimate the characteristic energy scale of these Kondo holes through a simple binary alloy model, consistent with the creation of Swiss cheese holes, in which the specific heat is composed of a superconducting and normal component:

$$C_{\text{tot}} = xC_N + (1-x)C_{\text{SC}}. \quad [1]$$

Because $C_{\text{tot}} \sim \ln(T^*/T)$ remains virtually unchanged with a Kondo lattice coherence temperature $T^* \sim 40$ K up to approximately 40% La in CeCoIn_5 (11), the large contribution to electronic specific heat from these Kondo holes ($\gamma_0 \sim 9.5$ J/mol La K^2 for $x = 0.1$; see Fig. 1) indicates that their effective mass is huge or, equivalently, that their characteristic energy scale is small, $T_{\text{KH}} = \pi R/6\gamma_0 \sim 0.3$ K for an effective “spin-1/2” La impurity, where R is the gas constant (12); strong scattering from these massive Kondo holes leads to the loss of quantum oscillations (13), even for <1% La impurities in CeCoIn_5 . Breaking the translational invariance of the Kondo lattice locally suppresses the superconducting gap significantly as seen in the strong reduction of the specific heat jump ΔC at T_c (Fig. 3A) of doped CeCoIn_5 , analogous to the strong temperature-dependent pair-breaking effects when Ce Kondo impurities, characterized by $T_K \sim 0.1$ K are introduced into the 3.3 K s -wave superconductor LaAl_2 (14); indeed, the suppression of ΔC in these two systems is very similar (Fig. 3A). Substitutions on the In site lead to either weaker suppression of the gap, or stronger suppression (Cd, Hg) possibly due to additional spin-flip pair-breaking effects caused by the local nucleation of magnetism near the Cd or Hg sites (15). Further support for the local suppression of superconductivity around the Kondo holes is provided by analysis of the effective size of an impurity bound state in a d -wave superconductor (4), given by $R_{\text{imp}} = \xi_0/(1 - \epsilon^2)^{1/2}$, where $\xi_0 = 4.9$ nm is the superconducting coherence length for the $\text{Ce}_{0.9}\text{La}_{0.1}\text{CoIn}_5$ sample, determined from the initial slope of the upper critical field dH_{c2}/dT_c (16). The ratio of the energy of the impurity state (or resonance) to the superconducting gap Δ_0 is $\epsilon_0 = \{[1 - (T_{\text{KH}}/0.3\Delta_0)^2]/[1 + (T_{\text{KH}}/0.3\Delta_0)^2]\}$ following ref. 17, where the strong-coupling value $\Delta_0 = 2.25T_c$ was used (6). From this formula, we find that $R_{\text{imp}} = 5.8$ nm is comparable to ξ_0 , using

$T_{\text{KH}} = 0.3$ K for $\text{Ce}_{0.9}\text{La}_{0.1}\text{CoIn}_5$, consistent with local suppression of superconductivity near the La impurities. [Similar impurity length scales $R_{\text{imp}} \sim \xi_0$ are obtained for other La concentrations $x = 0.02$ and 0.05 , which have nearly identical Kondo hole energy scales $T_{\text{KH}} \sim 0.2$ – 0.3 K (12) and values of dH_{c2}/dT_c (16).] Recent scanning-tunneling spectroscopy on Th impurities in URu_2Si_2 (18) reveals a strong local change of the density of states in this Kondo lattice, demonstrating that Kondo holes significantly affect the normal state as well (19). Our results further strengthen the connection between the heavy fermion superconductors and the cuprates, as the suppression of ΔC of Zn-doped YBCO is similar to that of $\text{Ce}_{1-x}\text{R}_x\text{CoIn}_5$ (Fig. 3A), and also to the iron-pnictide superconductors (20, 21), in which electronic inhomogeneity has been observed recently (22).

^{115}In nuclear quadrupole resonance (NQR) measurements further characterize the doping distribution of $\text{Ce}_{1-x}\text{La}_x\text{CoIn}_5$ and provide insight into the nature of the resulting electronic state. Fig. 4 shows the NQR signal for the $4\nu_Q$ quadrupolar ($\pm 9/2 \leftrightarrow \pm 7/2$) transition for the in-plane In(1), as well as the temperature dependence of the spin-lattice relaxation rates (T^{-1}_1) for $x = 0, 0.1$, and 1. The NQR peaks are relatively sharp in the pure compound (Fig. 4B) with the LaCoIn_5 frequency ($\nu_Q \sim 8.01$ MHz) smaller than that of CeCoIn_5 ($\nu_Q \sim 8.17$ MHz), in good agreement with previous reports (23, 24). The NQR spectrum in the normal state at $T = 3$ K is significantly broadened for the $x = 0.1$ sample, with the main peak (labeled A) virtually at the same frequency as in CeCoIn_5 and with two adjacent peaks (labeled B and C) resolved. There is no additional broadening or shift in the spectra as the sample becomes superconducting below $T_c = 0.9$ K, confirming that the heterogeneous electronic state below T_c has its origin in the normal state, as a result of doping. The lack of any intensity at the frequency corresponding to pure LaCoIn_5 and the similar temperature dependence of the spin-lattice relaxation rates of the three peaks—all with essentially the same onset T_c —rule out chemical segregation.

This thermodynamic analysis extends to other heavy fermion superconductors, as presented in Fig. 2B, and such electronic inhomogeneity may provide a framework for resolving several outstanding issues. In the 18.5 K superconductor PuCoGa_5 , the radioactive decay of Pu-239 produces defects and/or dislocations, mimicking the Swiss cheese hole in $\text{Ce}_{1-x}\text{R}_x\text{CoIn}_5$. Analysis of the specific heat data of a “fresh” (approximately 2-wk old)

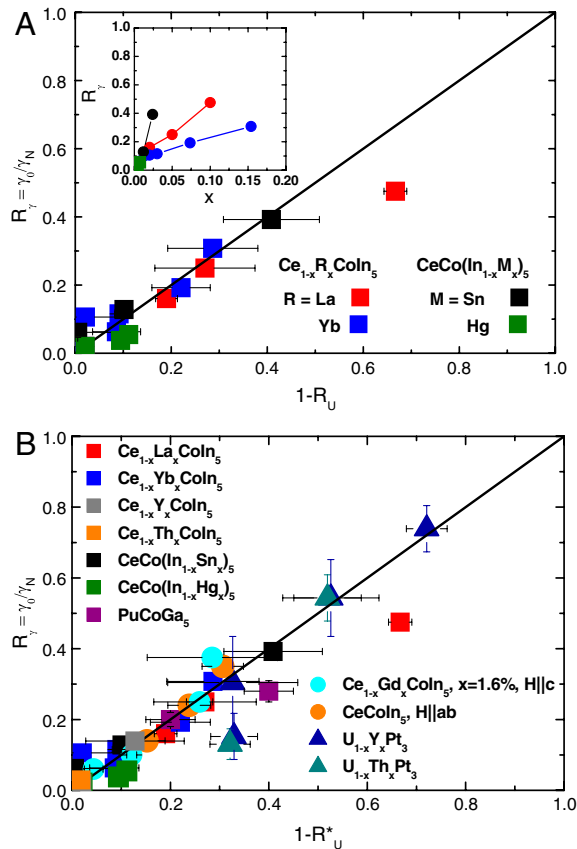


Fig. 2. Normal state fraction of the inhomogeneous heavy fermion ground state compared to the superconducting fraction of CeCoIn₅ with the introduction of nonmagnetic impurities and other heavy fermion systems at zero temperature. (A) Normal state fraction of the inhomogeneous heavy fermion ground state $R_y = \gamma_0/\gamma_N$ (determined from the C/T data in Fig. 1) of $Ce_{1-x}R_xCo(In_{1-y}M_y)_5$ ($R = La^{3+}, Yb^{2+}$; $M = Sn, Hg$) and superconducting state fraction, $1 - R_U$, where $R_U = [U_{SC}(x)/T_c^2(x)]/[U_{SC}(0)/T_c^2(0)]$, obtained from the superconducting condensation energy $U_{SC} = \int_0^{T_c} (S_N - S_S) dT$ (properly normalized relative to the condensation energy of pure CeCoIn₅). The linear relation between the two fractions indicates the superconductivity is excluded from a volume surrounding the impurity atom. (Inset) Linear variation of γ_0/γ_N as a function of impurity (La^{3+}, Yb^{2+}, Sn, Hg) concentration x . Error bars for R_y were obtained from a linear least-squares fit to the superconducting and normal state C/T data, whereas error bars for R_U were obtained from uncertainties in values of U_{SC} subject to entropy balance at T_c . In some cases, systematic errors in the entropy were corrected for using a procedure described in *Materials and Methods*. (B) Same as in A, including the unconventional superconductors $U_{1-x}M_xPt_3$ ($M = Th, Y$) and PuCoGa₅ (radiation damage-induced impurities), CeCoIn₅ and Ce_{0.994}Gd_{0.016}CoIn₅ in magnetic field, showing the general applicability of the analysis. The superconducting state fraction, $1 - R^*_U$, where $R^*_U = R_U/E_c$, with E_c comprising a small normalization factor to account for the γ_0 of the pure material as explained in *Materials and Methods*, is linear with respect to the normal state fraction, indicating the superconductivity is excluded from a volume surrounding the impurity atom, which implies an inhomogeneous electronic state. The parameters used in the analysis are given in Table S1. The lines in A and B are guides to the eye.

and “aged” (approximately 3-mo old) PuCoGa₅ sample (Figs. S3 and S4), reveals that the induced normal state fraction is comparable to the superconducting state fraction as radiation damage accumulates, in agreement with self-consistent T -matrix calculations describing the rate of suppression of T_c (20). Furthermore, the observed anomalous reduction in superfluid density (25) with time in this strong-coupling d -wave superconductor is similar to the reduction observed in the Zn-doped YBCO and LSCO cuprates (2). Likewise, nonmagnetic Y and Th impurities (26) introduced into the exotic (odd-parity, ref. 27) superconductor

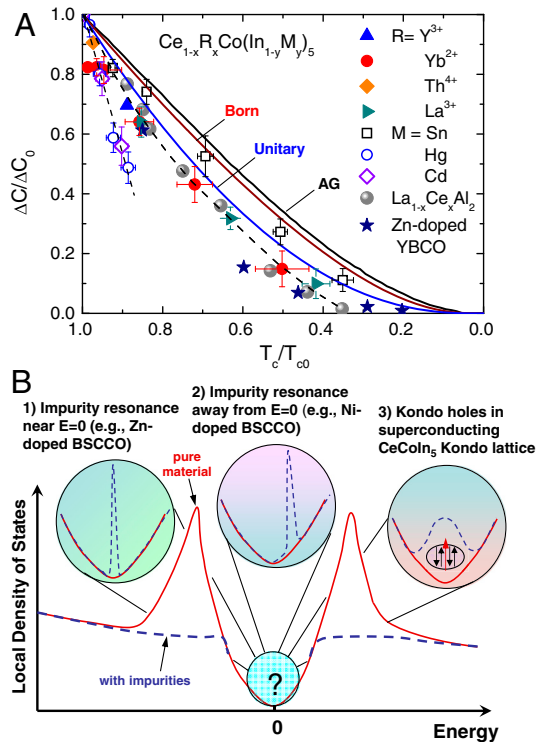


Fig. 3. Superconducting specific heat jump ΔC vs. T_c of $Ce_{1-x}R_x(In_{1-y}M_y)_5$ and $La_{1-x}Ce_xAl_2$, normalized to the values ΔC_0 and T_{c0} of the pure materials CeCoIn₅ and LaAl₂, and schematic of various novel inhomogeneous electronic states produced by impurities in cuprates and in CeCoIn₅. (A) Normalized superconducting specific heat jump $\Delta C/\Delta C_0$ vs. normalized transition temperature T_c/T_{c0} of $Ce_{1-x}R_x(In_{1-y}M_y)_5$, $La_{1-x}Ce_xAl_2$ (14), and Zn-doped YBCO (10). The black line is the Abrikosov-Gor’kov (AG) calculation for an s -wave Bardeen–Cooper–Schrieffer superconductor with magnetic impurities, and the blue and red lines are self-consistent T -matrix calculations for a d -wave superconductor with strong (unitary) or weak (Born) nonmagnetic scattering, respectively. The dashed lines are guides to the eye. Error bars for T_c for $Ce_{1-x}R_x(In_{1-y}M_y)_5$ were determined from the 10% and 90% values of $\Delta C/T$, and uncertainties in ΔC were determined from the entropy-conserving equal area construction. (B) Schematic of local density of states vs. energy E near the impurity showing three possible exotic forms of electronic inhomogeneity that emerge as intragap states of the unconventional superconductor, including (1) an impurity resonance located near $E = 0$ due to a strong scatterer [e.g., Zn impurities in Bi₂Sr₂CaCu₂O_{8- δ} (BSCCO)], (2) a resonance away from $E = 0$ due to an intermediate or weak scatterer (e.g., Ni impurities in BSCCO) and (3) proposed heavy Kondo hole (red arrow) that disrupts the superconducting CeCoIn₅ Kondo lattice (black arrows).

UPT₃ fall into this class of rather exceptional dopants. Finally, Tanatar et al. (28) have presented evidence for a normal component arising from an expansion of superconducting gap nodes on the Fermi surface in $Ce_{1-x}La_xCoIn_5$ ($x < 0.15$), a result interpreted within an extreme multiband model in which electrons with a small effective mass remain unpaired on small 3D Fermi surface pockets (for a different viewpoint, see ref. 29). In contrast to this scenario, a consistent picture emerges in which impurities (i) create an inhomogeneous electronic state within the superconducting condensate of CeCoIn₅ (Fig. 3B) and (ii) destroy the coherent Kondo lattice near the two-dimensional percolation limit, approximately 40% for the impurities (not the magnetic Ce ions), corresponding to a universal scattering rate given by a resistivity of $\rho_0 \sim 35 \mu\Omega cm$ (30). These novel states of matter within the Swiss cheese regions, which do far more than just suppress the superconducting gap, are ubiquitous in cuprates (4), but our study of this particular state reveals the nature of the underlying Kondo lattice and emphasizes the delicate interplay between unconventional superconductivity and the periodic array of Kondo ions from which it originates.

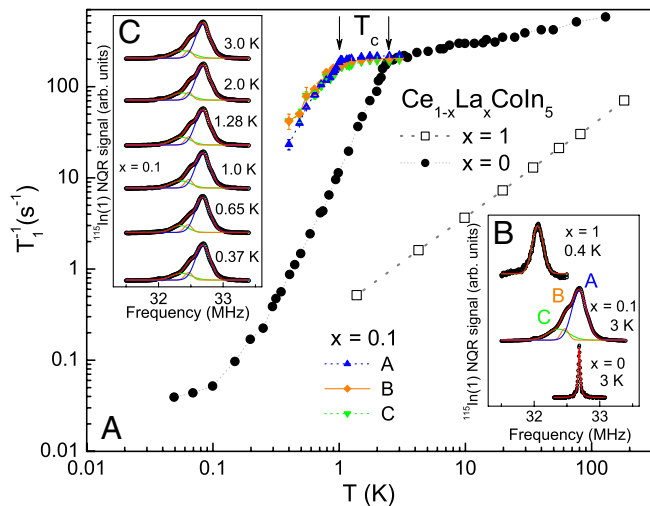


Fig. 4. $^{115}\text{In}(1)$ nuclear quadrupole resonance results in $\text{Ce}_{1-x}\text{La}_x\text{CoIn}_5$ for $x = 0, 0.1,$ and 1 . (A) Spin-lattice relaxation rate $1/T_1$ vs. temperature T . The $1/T_1$ data for $x = 1$ is from ref. 23 and for $x = 0$ from ref. 24. (B) $^{115}\text{In}(1)$ NQR spectra for the highest transition ($\pm 7/2 \leftrightarrow \pm 9/2$) at $T = 3$ K for $x = 0$ and 0.1 and at $T = 0.4$ K for $x = 1$. The solid lines are Gaussian ($x = 0.1$ and 1) and Lorentzian ($x = 0$) fits to the data. (C) $^{115}\text{In}(1)$ NQR spectra for $x = 0.1$ at several temperatures above and below $T_c \sim 0.9$ K. The solid lines are Gaussian fits to the data. The peaks A, B, C correspond to $\ln(1)$ with $0, 1,$ and 2 nearest-neighbor (nn) La, respectively; the relative intensities of the main peak (0.7) and the two satellites are 0.2 and 0.09 , reasonably close to the expected values for a simple binomial distribution [probabilities of 0.65 (0 nn), 0.29 (1 nn), and 0.05 (2 nn)], with a 10% chance of La occupying a Ce site. The error bars in A were determined from Gaussian fits to the data in C.

Our study of CeCoIn_5 and other heavy fermion superconductors highlights that superconductivity itself provides a previously unappreciated window on electronic inhomogeneity in Kondo lattice materials in the form of Kondo holes. Though some theoretical ideas have been put forth to investigate the disruption of the Kondo lattice by nonmagnetic impurities (7, 8), this problem remains virtually unexplored, aside from a few experimental studies (19, 31). Further investigations of Kondo holes in these f -electron Kondo lattices and superconductors, including the application of local probes such as scanning-tunneling spectroscopy, provide an opportunity to unravel their complexity; indeed, electronic inhomogeneity in these materials may well prove to be the norm rather than the exception.

Materials and Methods

Single crystals of $\text{Ce}_{1-x}\text{R}_x\text{Co}(\text{In}_{1-y}\text{M}_y)_5$ ($R = \text{Y}^{3+}, \text{La}^{3+}, \text{Gd}^{3+}, \text{Yb}^{2+}, \text{Th}^{4+}$; $M = \text{Sn}, \text{Cd}, \text{Hg}$) were grown from In flux, whereas single crystals of PuCoGa_5 were grown from Ga flux. Specific heat measurements were carried out in a Quantum Design Physical Properties Measurement System from 0.4 to 20 K (or from 5 to 25 K for PuCoGa_5), or in a $^3\text{He}/^4\text{He}$ dilution refrigerator from 50 mK to 3 K, in magnetic fields up to 9 T. The concentrations of the impurities were determined from energy-dispersive X-ray spectroscopy.

- Dagotto E (2005) Complexity in strongly correlated electronic systems. *Science* 309:257–262.
- Nachumi B, et al. (1996) Muon Spin Relaxation Studies of Zn-Substitution Effects in High-Tc Cuprate Superconductors. *Phys Rev Lett* 77:5421–5424.
- Pan SH, et al. (2000) Imaging the effects of individual zinc impurity atoms on superconductivity in $\text{Bi}_2\text{Sr}_2\text{CaCu}_2\text{O}_{8-\delta}$. *Nature* 403:746–750.
- Balatsky AV, Vekhter I, Zhu J-X (2006) Impurity-induced states in conventional and unconventional superconductors. *Rev Mod Phys* 78:373–433.
- Fisk Z, et al. (1988) Heavy-electron metals: New highly correlated states of matter. *Science* 239:33–42.
- Movshovich R, et al. (2001) Unconventional superconductivity in CeIrIn_5 and CeCoIn_5 : Specific heat and thermal conductivity studies. *Phys Rev Lett* 86:5152–5155.
- Sollie R, Schlottmann P (1991) A simple theory of the Kondo hole. *J Appl Phys* 69:5478–5480.
- Muller-Hartmann E, Zittartz J (1971) Kondo effect in superconductors. *Phys Rev Lett* 26:428–432.

The ^{115}In NQR measurements were performed using a phase coherent pulsed NMR/NQR spectrometer. Several crystals with similar T_c previously investigated by specific heat measurements were gently crushed into powder to improve the signal probed by the rf measurement. The frequency-swept ^{115}In NQR spectra ($I = 9/2$; $\gamma/2\pi = 9.3295$ MHz/T) were obtained using an auto-tuning probe in a ^3He cryostat. The spectra were obtained by stepwise summing the Fourier transform of the spin-echo signal. The values of the spin-lattice relaxation time T_1 were obtained by fits of the recovery of the nuclear magnetization $M(t)$ after a saturation pulse. The self-consistent T -matrix calculations of the specific heat jump are described in detail in ref. 32.

In our thermodynamic analysis, estimates of the normal state electronic specific heat coefficient γ_N were obtained by linear extrapolation to $T = 0$ K (a determination of γ_N obtained by fits of the data to the model of Moriya and Takimoto, ref. 33, for critical fermions yields similar values within 5–10%) and requiring entropy balance at T_c . The superconducting fraction of the heavy electrons is calculated by $R_U^* = U_{sc}/T_c^2/E_c$ where T_c is determined by equal entropy construction above and below T_c , U_{sc} is the superconducting condensation energy determined from the integration of the entropy difference between the normal (high field) and superconducting (zero field) states up to T_c , and E_c is a constant described below. If the high field data were not available for all doping levels, we used the normal state value for γ_N of the pure compound as an approximation for the doped compounds; the insensitivity of C/T just above T_c for all concentrations (Fig. 1) and the entropy balance at T_c indicate this approximation is reasonable. In a few cases ($x = 0.05$ La, 0.012 Sn, 0.03 Yb), the entropy balance was not satisfied in all available datasets (see Fig. 1); therefore, we added a small linear term (approximately 3–5% of γ_N) to correct the entropy balance and obtain two different values of U_{sc} before and after the correction for a better relative comparison within each doping series. We take the average and their difference gives the error bars for R_U of these samples in Fig. 2.

In our analysis of $\text{Ce}_{1-x}\text{R}_x\text{Co}(\text{In}_{1-y}\text{M}_y)_5$, we have taken approximately $E_c = U_{sc}(0)/T_c(0)^2$ from the pure compound CeCoIn_5 . This analysis, together with the experimental fact $R_\gamma + R_U = 1$ in Fig. 2, indicates that the pure compound of CeCoIn_5 has a negligible amount of impurities (i.e., comparing $\gamma_0 = 0.04$ J/mol · CeK^2 to $\gamma_N = 2$ J/mol · CeK^2). However, in some heavy fermion compounds such as $\text{U}_{1-x}\text{M}_x\text{Pt}_3$ and PuCoGa_5 , even the pure compounds have a significant number of defects or a large intrinsic γ_0 . In this case, it is necessary to define a parameter E_c , which corrects the normalization by $U_{sc}(0)/T_c^2(0)$ for additional disorder and/or systematic errors (see Table S1), to best fit all the doped data of a given system. For example, in PuCoGa_5 , $R_\gamma \sim 0.2$ even in the fresh sample, suggesting a large amount of defects caused by radiation damage, which is consistent with theoretical calculations that indicate $T_c = 19.1$ K in an undamaged material and account for the decrease in T_c with time (20, 25). In the case of UPt_3 , the pure material has a different condensation energy from the doped compounds (Fig. 2B), reflecting the double superconducting transition and also the sensitivity of this exotic odd-parity superconductor to impurities.

ACKNOWLEDGMENTS. Z.F. thanks Ilya Vekhter, Piers Coleman, and Lev Gor'kov for useful discussions and the hospitality of the Aspen Center for Physics. E.D.B. and J.D.T. thank H. Yasuoka for helpful discussions. This work was performed at Los Alamos National Laboratory under the auspices of the US Department of Energy, Office of Basic Energy Sciences, Division of Materials Sciences and Engineering. Work at University of California, Irvine was performed under the National Science Foundation (NSF) Grant NSF-DMR-0801253. Work at the National High Magnetic Field Laboratory was performed under the auspices of the NSF (DMR-0654118) and the State of Florida.

- Bianchi A, Movshovich R, Vekhter I, Pagliuso PG, Sarrao JL (2003) Avoided antiferromagnetic order and quantum critical point in CeCoIn_5 . *Phys Rev Lett* 91:257001.
- Loram JW, Mirza KA, Freeman PF (1990) The electronic specific heat of $\text{YBa}_2(\text{Cu}_{1-x}\text{Zn}_x)_3\text{O}_7$ from 1.6 K to 300 K. *Physica C* 171:243–256.
- Nakatsui S, et al. (2002) Intersite coupling effects in a Kondo lattice. *Phys Rev Lett* 89:106402.
- Rajan VT (1983) Magnetic susceptibility and specific heat of the Coqblin-Schrieffer model. *Phys Rev Lett* 51:308–311.
- Harrison N, et al. (2004) $4f$ -electron localization in $\text{Ce}_x\text{La}_{1-x}\text{MnIn}_5$ with $M = \text{Co}, \text{Rh},$ or Ir . *Phys Rev Lett* 93:186405.
- Luengo CA, Maple MB, Fertig WA (1972) Specific heat of the superconducting-Kondo system $(\text{La,Ce})\text{Al}_2$. *Solid State Commun* 11:1445–1450.
- Urbano RR, et al. (2007) Interacting antiferromagnetic droplets in quantum critical CeCoIn_5 . *Phys Rev Lett* 99:146402.
- Petrovic C, Bud'ko SL, Kogan VG, Canfield PC (2002) Effects of La substitution on the superconducting state of CeCoIn_5 . *Phys Rev B Condens Matter Mater Phys* 66:054534.

17. Satori K, Shiba H, Sakai O, Shimizu Y (1992) Numerical renormalization group study of magnetic impurities in superconductors. *J Phys Soc Jpn* 61:3239–3254.
18. Schmidt AR, et al. (2010) Imaging the Fano lattice to ‘hidden order’ transition in URu₂Si₂. *Nature* 465:570–576.
19. de la Torre AL, Visani P, Dalichaouch Y, Lee BW, Maple MB (1992) Th-doped URu₂Si₂: Influence of “Kondo holes” on coexisting superconductivity and magnetism. *Physica B* 179:208–214.
20. Curro NJ, et al. (2005) Unconventional superconductivity in PuCoGa₅. *Nature* 434:622–625.
21. Uemura YJ (2009) Superconductivity: Commonalities in phase and mode. *Nat Mater* 8:253–255.
22. Yin Y, et al. (2009) Scanning tunneling spectroscopy and vortex imaging in the iron pnictide superconductor BaFe_{1.8}Co_{0.2}As₂. *Phys Rev Lett* 102:097002.
23. Kohori Y, et al. (2001) NMR and NQR studies of the heavy fermion superconductors CeTln₅ (T = Co and Ir). *Phys Rev B Condens Matter Mater Phys* 64:134526.
24. Kawasaki Y, et al. (2003) Anisotropic spin fluctuations in heavy-fermion superconductor CeColn₅: In-NQR and Co-NMR studies. *J Phys Soc Jpn* 72:2308–2311.
25. Ohishi K, et al. (2007) Muon spin rotation measurements of the superfluid density in fresh and aged superconducting PuCoGa₅. *Phys Rev B Condens Matter Mater Phys* 76:064504.
26. Vorenkamp T, et al. (1993) Substitution studies and the nature of superconductivity in UPt₃. *Phys Rev B Condens Matter Mater Phys* 48:6373–6384.
27. Graf MJ, Yip SK, Sauls JA (2000) Identification of the orbital pairing symmetry in UPt₃. *Phys Rev B Condens Matter Mater Phys* 62:14393–14402.
28. Tanatar MA, et al. (2005) Unpaired electrons in the heavy-fermion superconductor CeColn₅. *Phys Rev Lett* 95:067002.
29. Seyfarth G, et al. (2008) Multigap superconductivity in the heavy-fermion system CeColn₅. *Phys Rev Lett* 101:046401.
30. Paglione J, Sayles TA, Ho PC, Jeffries JR, Maple MB (2007) Incoherent non-Fermi-liquid scattering in a Kondo lattice. *Nat Phys* 3:703–706.
31. Lawrence JM, et al. (1996) Kondo hole behavior in Ce_{0.97}La_{0.03}Pd₃. *Phys Rev B Condens Matter Mater Phys* 53:12559–12562.
32. Bauer ED, et al. (2006) Thermodynamic and transport investigation of CeColn_{5-x}Sn_x. *Phys Rev B Condens Matter Mater Phys* 73:245109.
33. Moriya T, Takimoto T (1995) Anomalous properties around magnetic instability in heavy electron systems. *J Phys Soc Jpn* 64:960–969.